

# CrashSniffer: UWB-Based Anchor-Free Pedestrian Collision Prediction for Personal Mobility Vehicles

Taeckyoung Lee, Juseung Lee<sup>†</sup>, Ryuhaerang Choi, Seungjoo Lee, Hyeongheon Cha, Hyungjun Yoon, Song Min Kim, Sangwook Bak<sup>§</sup>, and Sung-Ju Lee

KAIST, <sup>†</sup>Korea University, <sup>§</sup>Samsung Electronics  
Republic of Korea

{taeckyoung,ryuhaerang.choi,seungjoo.lee,hyeongheon,hyungjun.yoon,songmin,profsj}@kaist.ac.kr  
ljsjoa@korea.ac.kr,sangwook.bak@samsung.com

## Abstract

We present *CrashSniffer*, an anchor-free pedestrian collision prediction system for personal mobility (PM) vehicles such as e-scooters and e-bikes using Ultra-Wideband (UWB) sensing. *CrashSniffer* introduces a Virtual Antenna Array technique that harnesses the natural motion of PM vehicles to enhance localization accuracy without relying on external infrastructure. Coupled with a least-squares estimator, *CrashSniffer* enables pedestrian tracking under the challenging vehicle occlusion scenario. We then propose a Mobility-Aware Collision Prediction algorithm that considers pedestrian trajectories and directional intent to predict collisions. Field experiments demonstrate that *CrashSniffer* outperforms GPS and baseline UWB-based methods in pedestrian localization and collision prediction in realistic scenarios. Our scalable system offers a practical pathway to safer PM operation in pedestrian environments.

## CCS Concepts

• **Networks** → **Location based services**; • **Human-centered computing** → **Ubiquitous and mobile computing**.

## Keywords

Ultra-Wideband, Localization, Collision Prediction, Personal Mobility, Pedestrian Safety

---

Permission to make digital or hard copies of all or part of this work for personal or classroom use is granted without fee provided that copies are not made or distributed for profit or commercial advantage and that copies bear this notice and the full citation on the first page. Copyrights for components of this work owned by others than the author(s) must be honored. Abstracting with credit is permitted. To copy otherwise, or republish, to post on servers or to redistribute to lists, requires prior specific permission and/or a fee. Request permissions from [permissions@acm.org](mailto:permissions@acm.org).  
*EnvSys '25, Anaheim, CA, USA*

© 2025 Copyright held by the owner/author(s). Publication rights licensed to ACM.

ACM ISBN 979-8-4007-1986-8/25/06

<https://doi.org/10.1145/3742460.3742982>

## ACM Reference Format:

Taeckyoung Lee, Juseung Lee, Ryuhaerang Choi, Seungjoo Lee, Hyeongheon Cha, Hyungjun Yoon, Song Min Kim, Sangwook Bak, and Sung-Ju Lee. 2025. *CrashSniffer: UWB-Based Anchor-Free Pedestrian Collision Prediction for Personal Mobility Vehicles*. In *International Workshop on Environmental Sensing Systems for Smart Cities (EnvSys '25)*, June 23–27, 2025, Anaheim, CA, USA. ACM, New York, NY, USA, 6 pages. <https://doi.org/10.1145/3742460.3742982>

## 1 Introduction

Personal mobility (PM) vehicles such as e-scooters and e-bikes have rapidly grown in popularity, transforming urban transportation by offering convenient and eco-friendly mobility options. However, pedestrians often share sidewalks and crosswalks with these fast-moving PM vehicles, which frequently leads to collisions or near-misses [1]. This highlights a need to improve pedestrian safety around PM vehicles.

A key challenge arises when pedestrians are occluded from the rider's view, such as when they emerge behind parked vehicles. Vision-based systems like cameras and LiDAR often fail in these situations, as they can only detect pedestrians at the last moment. While RF-based alternatives such as GPS, Wi-Fi, and Bluetooth can penetrate occlusions, they suffer from low localization accuracy. Ultra-Wideband (UWB) offers both high ranging precision and robustness to multipath interference. However, most existing UWB approaches depend on pre-installed anchors, making them unsuitable for personal mobility (PM) vehicles, which typically lack dedicated infrastructure. This limitation highlights the need for a scalable, anchor-free localization solution in shared pedestrian environments.

To overcome these limitations, we propose *CrashSniffer*, a pedestrian collision prediction system for PM vehicles without any external anchors. *CrashSniffer* leverages UWB ranging between the PM and pedestrian, enhanced by a Virtual Antenna Array (VAA) that synthesizes a wider spatial baseline using the PM's natural motion. Building on the localization results, *CrashSniffer* further integrates a trajectory-aware collision prediction algorithm that estimates pedestrian intent and filters benign movements.

Our prototype *CrashSniffer* system, tested under realistic occlusion scenarios, achieved an average pedestrian localization error of only 1.00 m, outperforming GPS and UWB trilateration-based methods. With accurate localization, our algorithm predicts potential collisions with 0.93 F1-score. These findings demonstrate the potential of our lightweight, anchor-free UWB-based approach as a scalable and practical foundation for enhancing pedestrian safety in future urban mobility systems.

## 2 Related Work

Various localization techniques have been explored to support collision prediction between vehicles and pedestrians. GPS provides reliable positioning [5], but performs poorly in urban settings due to multipath effects. Approaches such as RTK/DGPS [9] were proposed to resolve this issue, but they incur high costs and infrastructure overhead. Alternatives using Wi-Fi [7], Bluetooth [3], and BLE [6] have been developed, but they suffer from lower time resolution and reduced ranging accuracy resulting from high signal noise and narrow bandwidths. Pedestrian Dead Reckoning (PDR) [4] improves GPS localization but accumulates drift over time.

UWB has recently achieved decimeter-level ranging errors in stationary conditions through time-of-flight measurements [2]. For instance, PedLoc [8] employs vehicle-mounted anchors to track pedestrians using overhearing-based UWB communication. Zhang et al. [11] demonstrated inter-vehicle localization through UWB-based vehicle-to-vehicle communication. Other works integrate UWB with IMU or PDR for challenging environments [10, 12]. While effective, existing approaches depend on fixed anchors, calibration, or pre-installed infrastructures that limit scalability in urban conditions.

In contrast, *CrashSniffer* introduces an anchor-free UWB localization system tailored for PM vehicles and pedestrians. By leveraging a VAA formed through the natural motion of the device, we estimate location without requiring fixed reference points. Our design offers accurate and scalable localization in infrastructure-limited environments.

## 3 CrashSniffer Overview

We propose *CrashSniffer*, a UWB-based system for pedestrian localization and collision prediction that operates without any pre-installed anchors. *CrashSniffer* first estimates the pedestrian's relative 2D position to a PM vehicle using Virtual Antenna Array-Enhanced Localization (V-Loc), which improves trilateration by leveraging motion-induced spatial resolution for robust accuracy under occlusion. Section 4.1 presents the baseline trilateration method, and Section 4.2 introduces V-Loc, which applies virtual antenna array over

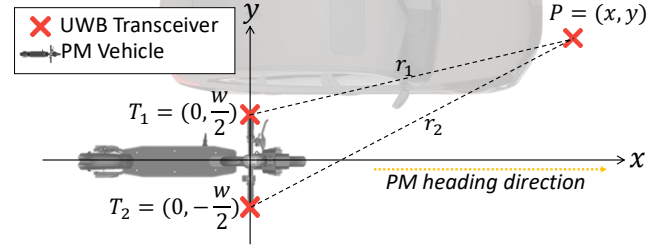


**Figure 1: Overview of trilateration-based localization of a pedestrian occluded behind a parked vehicle. Two UWB transceivers are placed on PM, and a pedestrian holds one transceiver. Ranging results  $(r_1, r_2)$  and a known distance between transceivers  $(w)$  are used to calculate the pedestrian position  $(x, y)$  via trilateration.**

multiple timestamps to improve estimation accuracy. Building on the localization results, Section 5 describes a mobility-aware collision prediction algorithm that anticipates actual threats while filtering out benign movements.

## 4 Anchor-Free Pedestrian Localization

*CrashSniffer* estimates a pedestrian's position relative to a PM vehicle using UWB ranging measurements. This section describes the underlying localization techniques, starting from a baseline trilateration method and extending to a motion-enhanced approach that leverages a virtual antenna array for improved accuracy under real-world conditions.

### 4.1 Trilateration-Based Localization

We localize pedestrians relative to the PM using UWB trilateration, with two transceivers on the PM's handlebars and one on the pedestrian. As more smartphones are equipped with UWBs, we expect the transceiver on pedestrians would be smartphones.

Figure 1 illustrates our approach. The PM moves along the  $x$ -axis, with transceivers ( $T_1$  and  $T_2$ ) at opposite ends of the handlebar with distance  $w$ , at  $(0, \pm \frac{w}{2})$ . The pedestrian is located at an unknown position  $P = (x, y)$ . Using single-sided two-way ranging, we measure the distances  $r_1$  and  $r_2$  from the pedestrian to  $T_1$  and  $T_2$ , respectively.

The pedestrian's position is estimated as the point where these two circles, centered at  $T_1$  and  $T_2$  with radii  $r_1$  and  $r_2$ , respectively, intersect:

$$x^2 + \left(y - \frac{w}{2}\right)^2 = r_1^2, \quad x^2 + \left(y + \frac{w}{2}\right)^2 = r_2^2. \quad (1)$$

We can easily derive the solution since the system comprises two equations with two unknowns. Subtracting these equations eliminates  $x^2$ :

$$\left(y - \frac{w}{2}\right)^2 - \left(y + \frac{w}{2}\right)^2 = r_1^2 - r_2^2 \Rightarrow y = \frac{r_2^2 - r_1^2}{2w}. \quad (2)$$

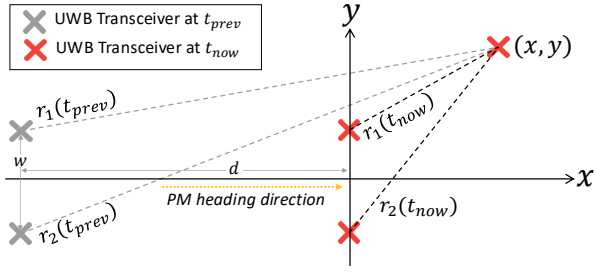


**Figure 2: Overview of VAA-enhanced localization (V-Loc).** V-Loc utilizes ranging results in two different timestamps ( $t_{prev}$  and  $t_{curr}$ ), PM moving distance ( $d$ ), and distance between transceivers ( $w$ ).

Substituting  $y$  back into the first equation, we solve for  $x$ :

$$x = \pm \sqrt{r_1^2 - \left(y - \frac{w}{2}\right)^2}. \quad (3)$$

*Challenges with Trilateration.* Trilateration offers a simple, anchor-free method for estimating the pedestrian’s lateral (side-to-side) position relative to the PM. However, it lacks the ability to resolve front-back ambiguity along the PM’s direction of motion. Additionally, its localization accuracy is highly sensitive to the inter-transceiver distance  $w$ ; specifically, the estimation error increases quadratically as  $w$  decreases (see Section 4.2). A smaller  $w$  amplifies the impact of ranging noise, necessitating a more robust approach.

## 4.2 Virtual Antenna Array-Enhanced Localization

To overcome the limitations of the trilateration-based approach, we introduce V-Loc, a VAA-enhanced localization method (Figure 2). While the original VAA concept assumes a static array of transceivers, we extend this idea to a dynamic setting by treating the same UWB transceiver at different timestamps as distinct virtual elements. By leveraging the forward motion of the PM vehicle, V-Loc effectively synthesizes a larger virtual array over time, thereby increasing spatial resolution and improving localization accuracy without additional hardware. Furthermore, VAA formulation resolves the front-back ambiguity along the  $x$ -axis, which the original trilateration approach cannot distinguish.

We consider a PM heading straight along the positive  $x$ -axis with a known speed. Two UWB devices are attached to the handlebar of the PM, positioned vertically at  $(0, \frac{w}{2})$  and  $(0, -\frac{w}{2})$ . Due to vehicle movement, these devices occupied positions  $(-d, \frac{w}{2})$  and  $(-d, -\frac{w}{2})$  at a previous time instance  $t - \Delta t$ . Thus, the virtual baseline  $d$  represents the horizontal displacement generated by the PM’s forward motion.

The pedestrian is positioned at unknown coordinates  $P = (x, y)$ . Leveraging VAA, we obtain UWB rangings in two different timings: current measurements ( $r_1(t_{curr})$  and  $r_2(t_{curr})$ ) and previous measurements ( $r_1(t_{prev})$  and  $r_2(t_{prev})$ ):

$$\begin{aligned} r_i^2(t_{prev}) &= (x + d)^2 + \left(y + (-1)^i \frac{w}{2}\right)^2, \\ r_i^2(t_{curr}) &= x^2 + \left(y + (-1)^i \frac{w}{2}\right)^2. \quad (i = 1, 2) \end{aligned} \quad (4)$$

As a result, we have four measurements with two variables ( $x, y$ ). While two equations are sufficient to obtain a closed-form solution for two unknowns, we minimize the residuals across all equations using the least-squares method for a more accurate and stable estimate, especially in noisy environments (e.g., vehicles between transceivers). Rewriting the equations in matrix form, we have:

$$\mathbf{A}\mathbf{x} = \mathbf{b}, \quad (5)$$

where

$$\mathbf{A} = \begin{bmatrix} 0 & -2w \\ 2d & 0 \\ 2d & -2w \\ 2d & 2w \end{bmatrix}, \mathbf{x} = \begin{bmatrix} x \\ y \end{bmatrix}, \mathbf{b} = \begin{bmatrix} r_1(t_{curr})^2 - r_2(t_{curr})^2 \\ r_1(t_{curr})^2 - r_1(t_{prev})^2 - d^2 \\ r_1(t_{curr})^2 - r_2(t_{prev})^2 - d^2 \\ r_2(t_{curr})^2 - r_1(t_{prev})^2 - d^2 \end{bmatrix}. \quad (6)$$

The pedestrian’s position  $(x, y)$  can thus be accurately estimated using the least-squares solution:

$$\hat{\mathbf{x}} = (\mathbf{A}^T \mathbf{A})^{-1} \mathbf{A}^T \mathbf{b}. \quad (7)$$

With the estimated position  $\hat{\mathbf{x}}$ , we keep track of the pedestrian’s position and apply the Extended Kalman filter to further suppress the error.

*Estimation Error Reduction from V-Loc.* We analyze the estimation error of the trilateration-based method and compare it with the error characteristics of our V-Loc approach.

Trilateration-based estimation of  $y_{Tri}$  is given in Eq. (2). Suppose each measured distance  $r_i$  is modeled as

$$r_i = r'_i + \epsilon_i, \quad (8)$$

where  $r'_i$  is the true distance and  $\epsilon_i \sim \mathcal{N}(0, \sigma^2)$  represents independent Gaussian noise with  $\sigma \ll r'_i$ . Then, the variance of the squared distance is approximated as:

$$\text{Var}(r_i^2) \approx 4r_i^2 \sigma^2. \quad (9)$$

Using Eq. (2), the variance of  $y_{Tri}$  becomes:

$$\text{Var}(y_{Tri}) = \frac{4r_1^2 + 4r_2^2}{4w^2} \sigma^2 = \frac{r_1^2 + r_2^2}{w^2} \sigma^2. \quad (10)$$

Assuming  $r_1 \approx r_2 \approx r$  for simplicity, Eq. (10) simplifies to:

$$\text{Var}(y_{Tri}) \approx \frac{2r^2}{w^2} \sigma^2. \quad (11)$$

For  $x_{Tri}$ , the sign ambiguity in Eq. (3) complicates the analysis. To enable the analysis, we ideally assume the positive

**Table 1: Comparison of position estimation variances between trilateration-based and V-Loc methods.**

	Var( $y$ )	Var( $x$ )
Trilateration	$2r^2\sigma^2/w^2$	$(r^2\sigma^2/x_{\text{Tri}}^2)(1/2 + 2y_{\text{Tri}}^2/w^2)$
V-Loc	$10r^2\sigma^2/9w^2$	$10r^2\sigma^2/9d^2$

sign for estimating  $x_{\text{Tri}}$ . We compute the variance of  $x$  considering that  $y$  is a function of  $r_1$  and  $r_2$ . Using the multivariate error propagation rule:

$$\text{Var}(x_{\text{Tri}}) = \left(\frac{\partial x_{\text{Tri}}}{\partial r_1}\right)^2 \sigma^2 + \left(\frac{\partial x_{\text{Tri}}}{\partial r_2}\right)^2 \sigma^2. \quad (12)$$

To calculate, we first derive  $x_{\text{Tri}}$  from Eq. (2) and Eq. (3):

$$x_{\text{Tri}} = \sqrt{r_1^2 - \left(\frac{r_2^2 - r_1^2}{2w} - \frac{w}{2}\right)^2}. \quad (13)$$

Then, using the chain rule:

$$\frac{\partial x_{\text{Tri}}}{\partial r_1} = \frac{r_1}{x_{\text{Tri}}} \left(\frac{1}{2} + \frac{y}{w}\right), \quad \frac{\partial x_{\text{Tri}}}{\partial r_2} = \frac{r_2}{x_{\text{Tri}}} \left(\frac{1}{2} - \frac{y}{w}\right). \quad (14)$$

Therefore, the full expression for the variance is:

$$\text{Var}(x_{\text{Tri}}) = \left(\frac{r_1}{x_{\text{Tri}}} \left(\frac{1}{2} + \frac{y_{\text{Tri}}}{w}\right)\right)^2 \sigma^2 + \left(\frac{r_2}{x_{\text{Tri}}} \left(\frac{1}{2} - \frac{y_{\text{Tri}}}{w}\right)\right)^2 \sigma^2. \quad (15)$$

Simplifying with  $r_1 \approx r_2 \approx r$  gives:

$$\text{Var}(x_{\text{Tri}}) \approx \frac{r^2\sigma^2}{x_{\text{Tri}}^2} \left(\frac{1}{2} + \frac{2y_{\text{Tri}}^2}{w^2}\right). \quad (16)$$

We now consider the V-Loc-based estimation in Eq. (7). We start from the least-squares solution  $\hat{\mathbf{x}} = (\mathbf{A}^\top \mathbf{A})^{-1} \mathbf{A}^\top \mathbf{b}$ . Here,  $(\mathbf{A}^\top \mathbf{A})^{-1} \mathbf{A}^\top$  is calculated as:

$$(\mathbf{A}^\top \mathbf{A})^{-1} \mathbf{A}^\top = \begin{bmatrix} 0 & \frac{1}{6d} & \frac{1}{6d} & \frac{1}{6d} \\ -\frac{1}{6w} & 0 & -\frac{1}{6w} & \frac{1}{6w} \end{bmatrix}. \quad (17)$$

The variances of  $x_{\text{V-Loc}}$  and  $y_{\text{V-Loc}}$  are calculated as:

$$\begin{aligned} \text{Var}(x_{\text{V-Loc}}) &= \text{Var}\left(\sum_i \left((\mathbf{A}^\top \mathbf{A})^{-1} \mathbf{A}^\top\right)_{1,i} \cdot b_i\right), \\ \text{Var}(y_{\text{V-Loc}}) &= \text{Var}\left(\sum_i \left((\mathbf{A}^\top \mathbf{A})^{-1} \mathbf{A}^\top\right)_{2,i} \cdot b_i\right). \end{aligned} \quad (18)$$

By calculating each  $x_{\text{V-Loc}}$ ,  $y_{\text{V-Loc}}$  with Eq. (18) and applying the variance of each  $r$  with simplification  $r_i \approx r$  results in:

$$\text{Var}(\hat{x}) \approx \frac{10r^2\sigma^2}{9d^2}, \quad \text{Var}(\hat{y}) \approx \frac{10r^2\sigma^2}{9w^2}. \quad (19)$$

Table 1 summarizes the estimated variances of V-Loc and the trilateration-based baseline. For the  $y$ -coordinate, V-Loc reduces the variance from  $2r^2\sigma^2/w^2$  to  $10r^2\sigma^2/9w^2$ . For the  $x$ -coordinate, the variance under trilateration depends on

both the measurement noise and the pedestrian position  $(x, y)$ , making it more sensitive to spatial configuration and noise propagation. In contrast, V-Loc yields a closed-form bound of  $10r^2\sigma^2/9d^2$ , which is not only tighter via a large PM moving distance  $d$  but also independent of  $x$  and  $y$ . These results demonstrate that V-Loc consistently achieves a more robust estimation than trilateration.

## 5 Mobility-Aware Collision Prediction

To complement the pedestrian localization algorithm V-Loc, *CrashSniffer* integrates a trajectory-aware collision prediction algorithm called MACP (Mobility-Aware Collision Prediction). MACP builds upon conventional sector-based collision detection methods [5] by incorporating pedestrian trajectory extrapolation and direction-aware filtering. This enables *CrashSniffer* to accurately distinguish between collision threats and benign pass-by movements, even under occlusion or blind spot scenarios.

To assess collision risk, we define a *probable area* as a forward-facing sector originating from the PM's current position, parameterized by a radius and angular span:

$$\theta = 2 \arctan\left(\frac{\alpha}{v}\right), \quad r = T \cdot v, \quad (20)$$

where  $v$  denotes the PM's speed,  $T$  is a tunable prediction horizon, and  $\alpha$  represents an empirically determined lateral safety margin (set to 2.334 [5]). This sector models the spatial extent of the PM's potential movement over time  $T$ . A pedestrian localized within this area using real-time UWB measurements is identified as a potential collision risk.

While the forward-facing sector captures the immediate risk area, it is insufficient in scenarios where pedestrians emerge abruptly, particularly from blind spots near the front of the PM, leaving little time for reaction. To address this issue, we perform linear extrapolation using the two most recent pedestrian positions, denoted as  $\mathbf{p}_{t-1}$  and  $\mathbf{p}_t$ , and predict an *estimated future position*  $\mathbf{p}_{t+1}$  as:

$$\mathbf{p}_{t+1} = \mathbf{p}_t + (\mathbf{p}_t - \mathbf{p}_{t-1}). \quad (21)$$

This extrapolated position  $\mathbf{p}_{t+1}$  is then used in place of  $\mathbf{p}_t$  for the sector inclusion test, enabling earlier detection of fast-approaching pedestrians whose current positions may lie just outside the predefined probable area.

To reduce false positives from non-collision cases (e.g., pedestrians passing by), we introduce an additional directional filter that checks whether the pedestrian's recent trajectory intersects a circular safety boundary around the PM. This boundary, with radius  $\rho = 0.7$  m, reflects the PM's physical footprint. The trajectory is modeled as a line segment  $\ell$  between  $\mathbf{p}_{t-1}$  and  $\mathbf{p}_t$ , and the perpendicular distance from

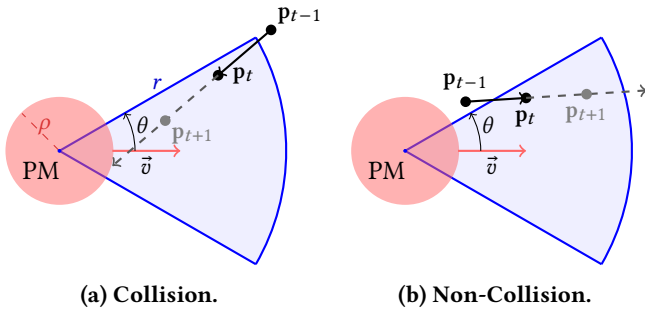


**Figure 3: Illustration of our mobility-aware collision prediction: (a) a colliding case and (b) a filtered non-colliding case.**

the PM’s position  $c$  to  $\ell$  is computed as:

$$d = \frac{|\mathbf{d} \times \mathbf{f}|}{|\mathbf{d}|}, \quad (22)$$

where  $\mathbf{d} = \mathbf{p}_t - \mathbf{p}_{t-1}$  and  $\mathbf{f} = \mathbf{p}_{t-1} - c$ . We predict the collision only if both the extrapolated position falls within the probable area and the trajectory  $\ell$  directs to PM with a certain threshold, i.e.,  $d \leq \rho$ .

Figure 3 illustrates the effectiveness of this direction-aware filtering. In the collision case (left), the pedestrian’s trajectory intersects the boundary and aligns with the PM’s direction of motion, satisfying both spatial and directional constraints. Conversely, the non-collision case (right) shows a pedestrian passing near the PM along a parallel path that does not intersect the critical zone. These examples highlight the importance of incorporating trajectory orientation into collision prediction, enabling the system to disregard non-threatening movements and focus on actual risks.

## 6 Experiments

### 6.1 Setup

We evaluate *CrashSniffer*, our anchor-free pedestrian collision prediction system, through controlled testbed experiments designed to reflect urban scenarios (Figure 4). The experimental setup replicates potential collisions between a PM vehicle and a pedestrian obscured by occlusion (e.g., parked vehicles).

To simulate PM operation, we use a remote-controlled vehicle equipped with two UWB transceivers mounted at handlebar height. The pedestrian is equipped with a handheld device, mimicking smartphone usage. Both PM and pedestrian devices are built using Raspberry Pi 4 units, integrated with UWB (Qorvo DWM3001C) and GPS (u-blox NEO-6M) modules.

For ground-truth localization, we employ a high-precision LiDAR sensor (Benewake TF03) and constrain movement paths using a custom rail track to ensure consistent positioning across trials. The PM accelerates from a stationary state,

**Table 2: Pedestrian localization error (m) under two pedestrian scenarios: standing (w/o collision) and crossing (w/ collision). Each averaged over seven rounds.**

	Standing	Crossing	Avg.
GPS	5.54±1.55	2.79±1.66	4.17±2.11
Trilateration	2.99±2.78	0.86±0.42	1.93±2.26
V-Loc (Ours)	<b>1.32±0.47</b>	<b>0.69±0.19</b>	<b>1.00±0.48</b>

reaching an average speed of 7.2 km/h, with an initial separation of 11 meters from the pedestrian. Each experiment concludes when the PM passes the potential collision point.

We test two pedestrian scenarios across multiple rounds: (1) Non-collision, the pedestrian stands still near the crossing point; and (2) Collision, the pedestrian crosses the PM’s path with limited visibility.

Throughout the experiment, V-Loc is used for real-time pedestrian localization, and MACP is applied to assess collision risk. Together, these components enable *CrashSniffer* to track pedestrian motion and predict collisions in real-time.

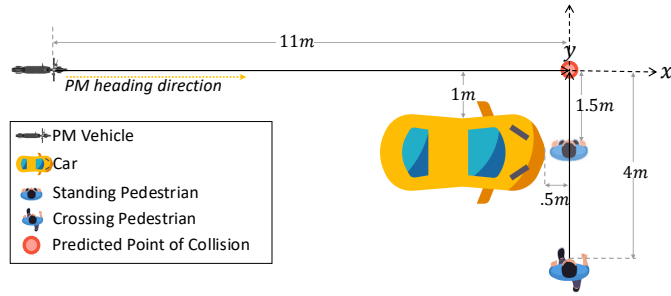
### 6.2 Results

**6.2.1 Relative Localization Performance.** To evaluate the accuracy of our UWB-based relative localization system, we performed seven rounds each for collision and non-collision scenarios. *CrashSniffer*’s performance was assessed by comparing the estimated positions of pedestrians relative to the PM vehicle against ground-truth measurements obtained via a high-precision LiDAR system.

Table 2 presents the average localization errors across both scenarios using three methods: GPS localization, UWB trilateration, and VAA-enhanced localization (V-Loc). Our approach achieved the lowest average localization error at  $1.00 \pm 0.48$  meters, significantly outperforming the GPS baseline ( $4.17 \pm 2.11$  meters) and the UWB trilateration method ( $1.93 \pm 2.26$  meters). The results validate our VAA-based localization’s improved accuracy and robustness, especially under dynamic occlusion conditions.

**6.2.2 Collision Prediction Performance.** We evaluated the collision prediction performance by measuring the ability of various systems to correctly identify potential collisions in challenging conditions such as occlusion. Metrics are true positive rate, true negative rate, and F1-score, with results reported in Table 3. We compare our system with the sector-based algorithm inspired by pSafety [5], predicting the collision when PM enters the safety zone.

By combining the collision prediction algorithm MACP with the localization algorithm V-Loc, *CrashSniffer* achieved the best-performing accuracy (F1=0.93), detecting  $1.33 \pm 0.29$  seconds before collision. This highlights *CrashSniffer*’s effectiveness in timely alerts with minimal false positives.



(a) Bird's-eye view of the experiment.



(b) Real-world scene with a pedestrian standing.

Figure 4: Experimental setup for evaluating UWB-based pedestrian collision prediction.

Table 3: Collision prediction performance. True positive/negative ratio (TPR/TNR) denotes accuracy for collision/non-collision experiments.

		TPR	TNR	F1
GPS	Sector-only	0.14	0.57	0.18
Trilateration	Sector-only	0.86	0.00	0.60
	MACP (Ours)	0.71	0.29	0.59
V-Loc (Ours)	Sector-only	1.00	0.00	0.67
	MACP (Ours)	1.00	0.86	<b>0.93</b>

In contrast, the sector-only baseline method often misclassifies situations where a pedestrian briefly enters the collision range but ultimately passes by without intersecting the PM's path. This leads to false positives and unnecessary alerts. Our MACP approach, by modeling pedestrian trajectory and motion direction, accurately distinguishes between true collision courses and non-threatening pass-by scenarios, ensuring only meaningful threats trigger warnings.

These results show the advantage of combining accurate localization with trajectory-aware prediction: *CrashSniffer* predicts true collisions and dynamically filters out benign interactions, improving safety without overwhelming users with false alarms.

## 7 Conclusion

We presented *CrashSniffer*, a novel UWB-based pedestrian collision prediction system for personal mobility vehicles, featuring a Virtual Antenna Array-based localization to enable accurate, anchor-free pedestrian tracking. Combined with our Mobility-Aware Collision Prediction algorithm, *CrashSniffer* reliably distinguishes between true collision risks and benign interactions by incorporating trajectory and directional cues. Experiments under occlusion conditions show *CrashSniffer* achieves 58% lower localization error and 39% higher F1-score compared with the best performing baselines.

As future work, we plan to extend the system beyond one-to-one communication to support multi-pedestrian tracking and evaluate its deployment in complex urban environments.

## Acknowledgments

This work was supported by Samsung Electronics Co., Ltd (IO210203-08381-01).

## References

- [1] J. B. Cicchino, P. E. Kulie, and M. L. McCarthy. Severity of e-scooter rider injuries associated with trip characteristics. *Journal of safety research*, 2021.
- [2] S. Fakhoury and K. Ismail. Improving pedestrian safety using ultra-wideband sensors: a study of time-to-collision estimation. *Sensors*, 2023.
- [3] R. Hasan, M. A. Hoque, Y. Karim, R. Griffin, D. C. Schwebel, and R. Hasan. Someone to watch over you: using bluetooth beacons for alerting distracted pedestrians. *IEEE internet of things journal*, 2022.
- [4] X. Hou and J. Bergmann. Pedestrian dead reckoning with wearable sensors: A systematic review. *IEEE Sensors Journal*, 2020.
- [5] C.-H. Lin, Y.-T. Chen, J.-J. Chen, W.-C. Shih, and W.-T. Chen. psafety: A collision prevention system for pedestrians using smartphone. In *2016 IEEE 84th Vehicular Technology Conference (VTC-Fall)*, 2016.
- [6] A. Mackey. *BLE Beacons for Proximity-Based and Location-Based Services*. PhD thesis, University of Guelph, 2019.
- [7] S. Mohammadi, K. Ismail, and A. H. Ghods. Investigating wi-fi, bluetooth, and bluetooth low-energy signal characteristics for integration in vehicle-pedestrian collision warning systems. *Sustainability*, 2021.
- [8] J. Park and Y.-B. Ko. Pedloc: Uwb-based pedestrian localization for autonomous vehicles. *Internet of Things*, 2024.
- [9] Q. C. Sun, J. C. Xia, J. Foster, T. Falkner, and H. Lee. Pursuing precise vehicle movement trajectory in urban residential area using multi-gnss rtk tracking. *Transportation research procedia*, 2017.
- [10] M. Wang, X. Chen, B. Jin, P. Lv, W. Wang, and Y. Shen. A novel v2v cooperative collision warning system using uwb/dr for intelligent vehicles. *Sensors*, 2021.
- [11] R. Zhang, L. Song, A. Jaiprakash, T. Talty, A. Alanazi, A. Alghafis, A. A. Biyabani, and O. Tonguz. Using ultra-wideband technology in vehicles for infrastructure-free localization. In *2019 IEEE 5th World Forum on Internet of Things (WF-IoT)*, 2019.
- [12] Y. Zhang, X. Tan, and C. Zhao. Uwb/ins integrated pedestrian positioning for robust indoor environments. *IEEE Sensors Journal*, 2020.